Coherently Enhanced Wireless Power Transfer

Editors' Suggestion | Featured in Physics

Coherently Enhanced Wireless Power Transfer

Alex Krasnok,[1] Denis G. Baranov,[2,3] Andrey Generalov,[4] Sergey Li,[5] and Andrea Alù[1,6,7,8,*]
[1]Department of Electrical and Computer Engineering, The University of Texas at Austin, Austin, Texas 78712, USA
[2]Department of Physics, Chalmers University of Technology, 412 96 Gothenburg, Sweden
[3]Moscow Institute of Physics and Technology, Dolgoprudny 141700, Russia
[4]Department of Electronics and Nanoengineering, Aalto University, 02150 Espoo, Finland
[5]ITMO University, St. Petersburg 197101, Russia
[6]Photonics Initiative, Advanced Science Research Center, City University of New York, New York 10031, USA
[7]Physics Program, Graduate Center, City University of New York, New York 10016, USA
[8]Department of Electrical Engineering, City College of The City University of New York, New York 10031, USA

(Received 3 December 2017; published 2 April 2018)

Extraction of electromagnetic energy by an antenna from impinging external radiation is at the basis of wireless communications and wireless power transfer (WPT). The maximum of transferred energy is ensured when the antenna is conjugately matched, i.e., when it is resonant and it has an equal coupling with free space and its load. This condition, however, can be easily affected by changes in the environment, preventing optimal operation of a WPT system. Here, we introduce the concept of coherently enhanced WPT that allows us to bypass this difficulty and achieve dynamic control of power transfer. The approach relies on coherent excitation of the waveguide connected to the antenna load with a backward propagating signal of specific amplitude and phase. This signal creates a suitable interference pattern at the load resulting in a modification of the local wave impedance, which in turn enables conjugate matching and a largely increased amount of extracted energy. We develop a simple theoretical model describing this concept, demonstrate it with full-wave numerical simulations for the canonical example of a dipole antenna, and verify experimentally in both near-field and far-field regimes.

DOI: 10.1103/PhysRevLett.120.143901

The antenna is a key element in wireless technology, including communications and power transfer [1–3]. While wireless communications are well established, wireless power transfer (WPT), proposed in the beginning of 20th century by Tesla [4], has been experiencing a rebirth in recent years. Demonstration of largely enhanced WPT efficiency in the near-field regime facilitated by resonant coupling [5] has opened novel opportunities for incorporation of WPT in various technologies, where recharging batteries without cables is of great importance. Examples include electric vehicles, implanted medical devices [6], and consumer electronics [7–9]. Significant research efforts have been recently devoted to exploring ways of achieving high WPT efficiency [10], optimizing the resonators' geometry [11], the surrounding materials [7,12,13], and their relative arrangement [5]. In addition, great progress has been recently made to ensure the overall robustness of near-field WPT systems against variations in the environment and background using active systems, nonlinearities, and feedback [14,15].

Recent research has shown that electromagnetic processes such as absorption and scattering may be effectively controlled via coherent spatial and temporal shaping of the incident electromagnetic field. For example, a coherent perfect absorber is a linear electromagnetic system, in which perfect absorption of radiation is achieved with two or more incident coherent waves, creating constructive interference inside an absorbing structure [16–19]. Similar principles also allow developing linear logic gates [20], recognition setups [21], and achieving "virtual" absorption in transparent systems [22], in which interference between two input waves is the enabling factor.

In this Letter, we propose a conceptually different approach to realize robust WPT systems, which relies on the local control of the wave impedance offered by interference phenomena, in analogy with coherent perfect absorbers. We show that this approach can be employed to improve and control dynamically the matching of receiving antennas, and as a result enhance the performance of WPT systems overcoming changes in the channel link between transmitter and receiver. Specifically, we demonstrate that there is a possibility to improve the receiving efficiency of an antenna by coherent excitation of the out-coupling waveguide with a backward propagating signal of a proper amplitude and phase, Fig. 1. This signal creates a specific interference pattern in the system that results in optimal wave impedance at the feed location, maximizing the energy transferred to the receiving antenna from free space.

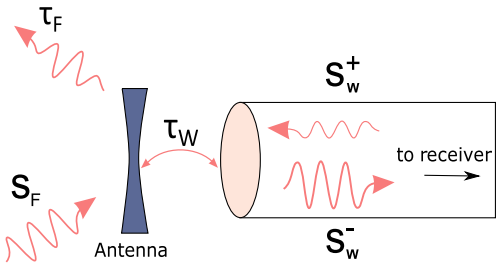

FIG. 1. Sketch of a coherently enhanced WPT system. The incident radiation (s_F) excites the antenna, which reradiates back into free space at a rate $1/\tau_F$ and couples to the waveguide at a rate $1/\tau_w$ creating a forward-propagating waveguide mode (s_w^-). Coherent excitation of the waveguide with a backward propagating mode (s_w^+) with a specific amplitude and phase can retune the matching condition and largely improve the WPT performance.

We develop an illustrative analytical model predicting this effect, demonstrate it in full-wave numerical simulations, and in a microwave experiment.

In order to demonstrate the effect of coherently enhanced power transfer, we develop a theoretical model on the basis of temporal coupled mode theory [23,24], which applies for both near-field and far-field WPT systems. The system of a waveguide-coupled antenna is schematically shown in Fig. 1. The antenna is excited by a field s_F created by a transceiver, which can be either free-propagating or evanescent. The antenna, in turn, excites the waveguide mode with amplitude s_w^-, which carries the out-coupled energy to the load. To model the structure, we will assume that the antenna has a single resonance at the operating frequency ω_0. The dynamics of the resonant mode amplitude a are described by the equation [23,24]

$$\frac{da}{dt} = (i\omega_0 - 1/\tau)a + \langle \kappa^* | s_+ \rangle, \tag{1}$$

where τ is the mode damping time, $|\kappa\rangle = (\kappa_w, \kappa_F)$ is the coupling constants vector, and $|s_+\rangle = (s_w^+, s_F)$ is the input amplitudes vector. The output amplitude vector $|s_-\rangle$, on the other hand, is related to the input vector and the resonance amplitude via

$$|s_-\rangle = \hat{C}|s_+\rangle + a|\kappa\rangle, \tag{2}$$

where $\hat{C}$ is the direct scattering matrix, which reflects the direct pathway between input and output channels.

The two crucial parameters that determine the system response are τ_w and τ_F, being the antenna decay times into the waveguide mode and into radiation in free space, respectively. If the antenna does not exhibit large Ohmic losses (which is a reasonable assumption in the microwave region), the total decay time is given by $1/\tau = 1/\tau_w + 1/\tau_F$. The coupling constants are related to the corresponding decay times as $\kappa_w = \sqrt{2/\tau_w}$ and $\kappa_F = \sqrt{2/\tau_F}$ [24]. The direct scattering matrix, in turn, satisfies $\hat{C}|\kappa\rangle^* = -|\kappa\rangle$ [24].

Equations (1) and (2) establish the relation between the continuum of free-space modes and the discrete waveguide mode. The goal of efficient WPT is to enhance the amplitude of the backscattered waveguide mode, denoted by s_w^- in Fig. 1. Therefore, for the sake of simplicity, we reduce the direct scattering matrix to a scalar c, assuming that the coupling of the antenna with free-space modes leading to additional radiation losses is taken into account by τ_F. Such simplification does not undermine our model. Furthermore, for a microwave waveguide or a coaxial cable it may be safely assumed that there is no direct scattering from the waveguide into free space (i.e., this interaction is mostly mediated by the antenna). Therefore, $c = -\kappa_w/\kappa_w^* = -1$, and the resulting amplitude of the reflected mode that carries the transferred energy is given by

$$s_w^- = cs_w^+ + \kappa_w \frac{\kappa_w s_w^+ + \kappa_F s_F}{i(\omega - \omega_0) + 1/\tau}. \tag{3}$$

With $s_F = 0$ this expression yields the reflection s parameter (s_{11}) that can be easily measured experimentally or calculated numerically.

In the passive case ($s_w^+ = 0$) this expression results in a conventional Lorentzian spectrum for the transferred energy $|s_w^-|^2$, reaching a maximum at the resonant frequency ω_0, see Fig. 2(a), where the calculations are presented for amplitude of the impinging free space mode $|s_F| = 1$. This maximum can be easily found from Eq. (3) and it is equal to $4\tau_w\tau_F/(\tau_w + \tau_F)^2$. The optimal condition for coupling of the incident free space mode into the waveguide is known as the critical coupling, or conjugate matching condition [1], and it is achieved when $\tau_w = \tau_F$. This condition maximizes the amount of energy transmitted into the waveguide at resonance. While it is always possible to design the antenna so that the load resistance balances the radiation resistance to satisfy this condition, in practice as the environment, or generally the channel connecting transmitter and receiver, change, the load needs to be retuned to satisfy the conjugate matching condition. In the following, we show that it is possible to maximize transmission without affecting the coupling parameters and retune the conjugate matching condition in real time by coherent illumination of the antenna from the loading port, similarly to the concept of coherent perfect absorption, when critical coupling for absorption in an unbalanced system is restored by an impinging coherent wave with proper phase and amplitude [16,19].

We now inspect how an auxiliary back-propagating wave impinging from the waveguide port at the load of the antenna modifies the input-output characteristic of the system in the active case. In Fig. 2(b) we show the energy balance $\Sigma = |s_w^-|^2 - |s_w^+|^2$ of transferred energy as a function of the auxiliary power $|s_w^+|^2$ for different values of the relative phase $\varphi = \mathrm{Arg}(s_w^+/s_F)$. Choosing the energy balance as a metric allows us to treat far-field and near-field

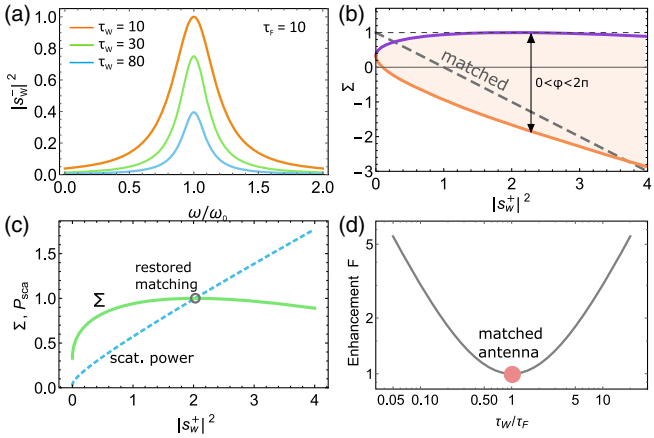

FIG. 2. Analytical modeling of coherently enhanced WPT. (a) Spectrum of the transferred energy ($|s_w^-|^2$) in the passive case (no back-propagating signal) for antennas with different waveguide couplings. The decay times are measured in the units of $1/\omega_0$. (b) Energy balance Σ for a resonant matched (gray dashed curve) and resonant mismatched antenna with $\tau_F = 10$ and $\tau_w = 100$ (color solid curves). Solid area indicates the region of available values of the energy balance. (c) Energy balance and total power scattered by the mismatched antenna P_{sca} for the optimal phase of the auxiliary mode. The two values are equal at the point of restored conjugate matching. (d) Enhancement factor F defined as the ratio of maximal achievable energy balance assisted by the auxiliary signal to the transferred energy $|s_w^-|^2$ without coherent illumination as a function of τ_w/τ_F.

WPT systems on an equal footing. A positive (negative) energy balance indicates that the antenna receives (radiates) more energy than radiates (receives). More importantly, if the energy balance exceeds the receiving energy $|s_w^-|^2$ in the passive case ($|s_w^+|^2 = 0$), it signifies more favorable coherently assisted performance of the WPT system. One can also define efficiency of the coherently enhanced WPT system as $\Sigma/P_{\text{tr}}^{\text{rad}}$, where $P_{\text{tr}}^{\text{rad}}$ is the total power radiated by the transceiver. Definition and optimization of this quantity, however, requires knowledge of the transceiver layout, whereas the goal of this work is the optimization of the energy balance Σ by means of coherent excitation.

For an antenna that is already conjugate matched (gray dashed line), as expected, the maximal power transfer arises when the auxiliary signal from the port is absent, since this signal would only detune the already optimal matching condition. This curve does not depend on the relative phase since the signal s_w^+ does not reflect back and, hence, does not alter the total receiving energy $|s_w^-|^2$. However, for a mismatched antenna (filled region in the plot) the input-output characteristic exhibits a peculiar behavior. The filled region marks all achievable values of the energy balance for phase differences spanning the whole range between 0 and 2π, indicating that for a suitable combination of phase and amplitude the energy balance exceeds that of the passive case, even after subtracting the energy carried by the back-propagating signal. In particular, for a certain phase difference the energy balance (purple curve) reaches the ideal value of a resonant critically coupled antenna. Coherent illumination therefore restores the critical waveguide-antenna coupling, without having to retune the antenna load impedance. The specific value of optimal phase that ensures critical coupling depends on the direct scattering matrix $\hat{C}$; if we allow direct pathways between the free space and the waveguide, or a reactive mismatch of the load, the phases of reflected and transmitted waves would be different and the optimal phase difference would change. Remarkably, in the regime of restored critical coupling not only the energy balance Σ is maximized, but it also exactly equals the power scattered by the antenna into free space, $P_{\text{sca}} = 2|a|^2/\tau_F$; see Fig. 2(c).

To better illustrate the capabilities of this approach, we show in Fig. 2(d) the enhancement factor $F = \max \Sigma/|s_w^-(s_w^+ = 0)|^2$, where $s_w^-(s_w^+ = 0)$ denotes the amplitude of the s_w^- mode in the passive case. It is seen that for a critically coupled system $F = 1$, since the energy balance cannot be increased by the auxiliary mode. For a mismatched antenna, on the other hand, the coherence-assisted enhancement factor increases with deviation of τ_w/τ_F from 1, and, therefore, can have large values for strongly mismatched antennas. In the radio frequency range, mismatched and nonresonant antennas are common in the context of various wireless charging devices, in which the antenna, of cm scale length, is far off-resonant, since the radiation of the wireless transfer platform is lying in the 100 kHz range [10]. Our approach allows tuning the antenna to the optimal condition through wave interference. In addition, in many situations the matching condition can be easily spoiled by changes in the environment, such as parasitic reflections, or by a changing distance to the transmitter. Our approach offers a viable solution to real-time retuning of the antenna by sending a signal from the receiving port to modify the local wave impedance at the load.

To verify the predictions of the analytical model, we carried out FDTD simulations of coherently enhanced WPT using the CST MICROWAVE STUDIO. In our model, a coaxial cable was coupled to a nonresonant dipole antenna with 5 cm arm length. Microwave radiation at 1.36 GHz (with a wavelength of 22 cm) from the open end of a rectangular waveguide separated by a distance of 40 cm from the antenna was used as the incident radiation (s_F). A coherent auxiliary signal (s_w^+) was launched into the coaxial cable in order to enable the interference. The resulting dependence of the energy balance shown in Fig. 3(a) reproduces the theoretical predictions. We note that the relative phase denoted here as ϕ is calculated for the $\text{Arg}(s_w^+)$ and $\text{Arg}(s_F)$ taken at different points (at the dipole antenna center and at the rectangular waveguide end, respectively) and, hence, depends on their relative distance.

To provide more insight into the observed behavior, we present in Figs. 3(b),3(c) the Poynting vector distribution

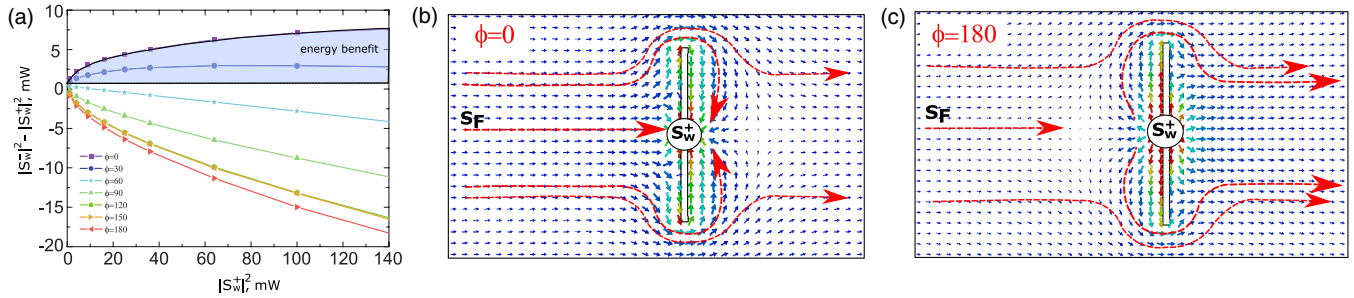

FIG. 3. Numerical simulations of the proposed approach of coherently enhanced WPT for the canonical example of a dipole antenna. (a) Energy balance ($|s_w^-|^2 - |s_w^+|^2$) as a function of the auxiliary signal intensity ($|s_w^+|^2$) for different relative phase values. The black dashed line shows the energy level received by the dipole antenna without auxiliary signal. Solid area indicates the region of energy benefit, where the coherently assisted energy balance exceeds that for $s_w^- = 0$. (b),(c) Poynting vector distribution around the microwave antenna with the auxiliary signal of amplitude $|s_w^+| = 12$ and relative phases of 0° (b) and 180° (c).

around the antenna considering the coherent excitation with relative phases of 0° [Fig. 3(b)] and 180° [Fig. 3(c)]. It is evident that, when the antenna is coherently excited by a wave of appropriate amplitude and phase, it enables largely enhanced antenna aperture that collects more energy into the coaxial cable from the propagating wave, Fig. 3(b). On the other hand, when the relative phase is not well chosen, the external wave (s_F) enables enhanced radiation of the dipole antenna into free space.

Finally, we perform a proof-of-principle experiment to demonstrate the feasibility of coherently enhanced WPT.

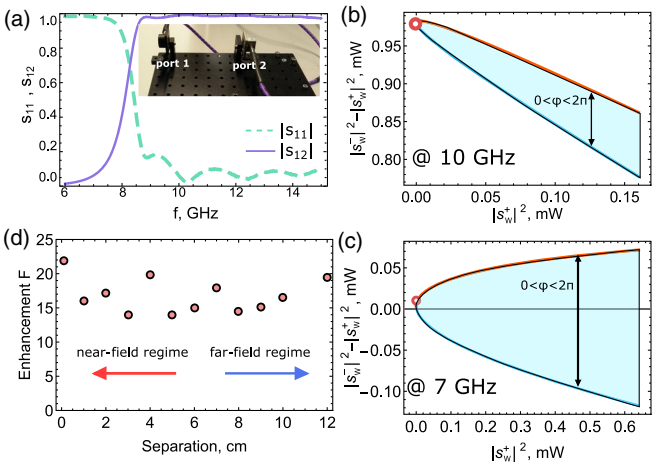

FIG. 4. Experimental verification of coherently enhanced wireless energy transfer. (a) Measured spectrum of s_{11} and s_{22} absolute values for transmitting and receiving antennas placed next to each other. Inset: Photo of the experimental setup. Two coaxial cables are attached to the vector network analyzer ports and terminated with waveguide to coaxial adapters at the free ends. One port serves as the transmitter, while the other serves as the power receiver. (b),(c) The energy balance $|s_w^-|^2 - |s_w^+|^2$ vs power of the additional signal $|s_w^+|^2$ for two different frequencies. The shaded area corresponds to all values of the relative phase between the external signal and the auxiliary mode. The power of 1 mW is fed to port 1 in both cases. (d) Dependence of the energy transfer enhancement factor F on the distance between the WCAs at fixed frequency of 7 GHz.

For this purpose, we put together a microwave two-port system shown in the inset of Fig. 4(a). Each coaxial cable is connected to a vector network analyzer and terminated with a waveguide to coaxial adapter (WCA) that transforms electrical currents to propagating electromagnetic radiation. Figure 4(a) presents the absolute values of measured s_{11} and s_{12} scattering parameters for arrangement of the system with the WCA placed next to each other. The WCAs have cutoff frequency around 8 GHz, which manifests itself in high reflection (s_{11}) at frequencies below 8 GHz. Thus, the WCA operates as a mismatched antenna for frequencies below 8 GHz and an almost matched antenna for frequencies above 8 GHz. The port 1 creates free space radiation s_F, a part of which (s_w^-) is then received by port 2. Port 2 is excited by the auxiliary signal (s_w^+) of variable amplitude and phase.

The resulting s-parameter spectra allow us to observe coherently enhanced energy transfer. The dependence of the energy balance Σ vs power of the additional excitation $|s_w^+|^2$ for the whole set of relative phases $0 < \phi < 2\pi$ presented in Figs. 4(b) and 4(c) highlights the different behavior of the system in various spectral regions. At 10 GHz, where reflection by each WCA back to the coaxial cable is very low, excitation with the auxiliary signal barely improves the energy transfer, Fig. 4(b). At 7 GHz, however, the situation is strikingly different: high reflection by the WCA enables order of magnitude enhancement of the transferred power, Fig. 4(c). This enhancement becomes possible due to a small transmission from port 1 to port 2 even at 7 GHz, which can be increased by interference with the auxiliary signal.

To further inspect the opportunities offered by coherently enhanced energy transfer, we study the input-output behavior of our setup for different distances between the WCAs. Figure 4(d) shows the enhancement factor F versus the distance at the fixed frequency of 7 GHz (wavelength of 4.28 cm), where the WCAs operate as largely mismatched antennas. At each distance, the maximum of F is achieved for a specific relative phase between the two signals, which is determined by complex values of s parameters for the given arrangement of the setup. An enhancement of the received

energy around 20 can be achieved at this frequency for the whole range of distances (0–12 cm, which covers both the near- and far-field regimes), highlighting the great versatility of the present approach for both near-and far-field WPT systems, and the possibility or realizing robust WPT independent of variations of the distance between transmitter and receiver.

We envision that in a practical WPT device, one may control in real time the amplitude and phase of the auxiliary signal to retune the antenna as a function of changes in the environment, temperature changes in the load, and distance of the transmitter. We propose the employment of an adaptive filter in the receiver circuit that monitors the transferred power and self-adjusts the amplitude and phase of the auxiliary signal such that it maximizes in real-time the transferred power. In order to reduce the time needed to find an optimal condition, we may estimate a "seed" value of the auxiliary wave amplitude. By equating $d\Sigma$ to zero, we find the optimal value of the auxiliary wave amplitude $s_{\mathrm{opt}}^{+}=-s_{w}^{-}(s_{w}^{+}=0)[R/(R+1)(R-1)]$, where $R=(2\tau/\tau_{w})-1$ is the reflection coefficient for the back-propagating wave at resonance [see Eq. (3) with $\omega=\omega_0$], which can be measured experimentally for the specific realization.

In conclusion, we have shown that coherent signals sent from the receiving port of a WPT system can largely enhance and control the power transfer efficiency. This additional signal creates a tailored interference in the system, modifying the local wave impedance at the antenna load, thus enabling conjugate matching and critical coupling even if the antenna itself is largely mismatched, resulting in an increased amount of energy extracted to the waveguide from free space. We have developed an illustrative analytical model predicting this effect and demonstrated it in numerical simulations and in a microwave experiment. Our approach of coherently enhanced WPT can be applied for the development of efficient wireless power transfer systems with robust operation in rapidly changing environments, as common in practical situations and setups.

The authors are grateful to Professor Constantin Simovski and Professor Sergei Tretyakov for their expert advice and helpful criticism during the elaboration of this work. This work was partially supported by the Air Force Office of Scientific Research with MURI Grant No. FA9550-17-1-0002, the National Science Foundation, the Samsung GRO program, the Simons Foundation, and Knut and Alice Wallenberg Foundation.

*alu@mail.utexas.edu

[1] C. A. Balanis, *Antenna Theory: Analysis and Design* (John Wiley & Sons, New York, 1997).
[2] M. Agio and A. Alú, *Optical Antennas* (Cambridge University Press, Cambridge, England, 2013).
[3] L. Novotny and B. Hecht, *Principles of Nano-Optics* (Cambridge University Press, Cambridge, England, 2012).
[4] W. C. Brown, IEEE Trans. Microwave Theory Tech. **32**, 1230 (1984).
[5] A. Kurs, A. Karalis, R. Moffatt, J. D. Joannopoulos, P. Fisher, and M. Soljacic, Science **317**, 83 (2007).
[6] J. S. Hoa, A. J. Yeha, E. Neofytoub, S. Kima, Y. Tanabea, B. Patlollab, R. E. Beyguib, and A. S. Y. Poon, Proc. Natl. Acad. Sci. U.S.A. **111**, 7974 (2014).
[7] S. Kim, J. S. Ho, and A. S. Y. Poon, Phys. Rev. Lett. **110**, 203905 (2013).
[8] H. Mei and P. P. Irazoqui, Nat. Biotechnol. **32**, 1008 (2014).
[9] S. Kim, J. S. Ho, L. Y. Chen, and A. S. Y. Poon, Appl. Phys. Lett. **101**, 073701 (2012).
[10] M. Song, P. Belov, and P. Kapitanova, Appl. Phys. Lett. **4**, 021102 (2017).
[11] M. Song, I. Iorsh, P. Kapitanova, E. Nenasheva, and P. Belov, Appl. Phys. Lett. **108**, 023902 (2016).
[12] B. Wang, K. H. Teo, T. Nishino, W. Yerazunis, J. Barnwell, and J. Zhang, Appl. Phys. Lett. **98**, 254101 (2011).
[13] Y. Urzhumov and D. R. Smith, Phys. Rev. B **83**, 205114 (2011).
[14] S. Assawaworrarit, X. Yu, and S. Fan, Nature (London) **546**, 387 (2017).
[15] Y. Ra'di, C. A. Valagiannopoulos, A. Alú, C. R. Simovski, and S. A. Tretyakov, arXiv:1705.07964.
[16] Y. D. Chong, L. Ge, H. Cao, and A. D. Stone, Phys. Rev. Lett. **105**, 053901 (2010).
[17] Y. D. Chong, L. Ge, and A. D. Stone, Phys. Rev. Lett. **106**, 093902 (2011).
[18] J. Zhang, K. F. MacDonald, and N. I. Zheludev, Light Sci. Appl. **1**, e18 (2012).
[19] D. G. Baranov, A. Krasnok, T. Shegai, A. Alú, and Y. D. Chong, Nat. Rev. Mater. **2**, 17064 (2017).
[20] X. Fang, K. F. MacDonald, and N. I. Zheludev, Light Sci. Appl. **4**, e292 (2015).
[21] M. Papaioannou, E. Plum, and N. I. Zheludev, ACS Photonics **4**, 217 (2017).
[22] D. G. Baranov, A. Krasnok, and A. Alù, Optica **4**, 1457 (2017).
[23] H. Haus, *Waves and Fields in Optoelectronics* (Prentice Hall, Englewood Cliffs, NJ, 1984).
[24] S. Fan, W. Suh, and J. D. Joannopoulos, J. Opt. Soc. Am. B **20**, 569 (2003).